8. Iordanskii S V, Lyanda-Geller Yu B, Pikus G E *Pis'ma Zh. Eksp. Teor. Fiz.* **60** 199 (1994) [*JETP Lett.* **60** 206 (1994)]
9. Knap W et al. *Phys. Rev. B* **53** 3912 (1996)
10. Studenikin S A et al. *Phys. Rev. B* **68** 035317 (2003)
11. Golub L E *Phys. Rev. B* **71** 235310 (2005)
12. Guzenko V A et al. *Phys. Status Solidi C* **3** 4227 (2006)
13. Yu G et al. *Phys. Rev. B* **78** 035304 (2008)
14. Glazov M M, Golub L E *Semicond. Sci. Technol.* **24** 064007 (2009)
15. Glazov M M, Golub L E *Fiz. Tekh. Poluprovodn.* **40** 1241 (2006) [*Semiconductors* **40** 1209 (2006)]
16. Gurioli M et al. *Phys. Rev. Lett.* **94** 183901 (2005)
17. Glazov M M, Golub L E *Phys. Rev. B* **77** 165341 (2008)
18. Glazov M M, Golub L E *Phys. Rev. B* **82** 085315 (2010)
19. Amo A et al. *Phys. Rev. B* **80** 165325 (2009)
20. Ganichev S D et al. *J. Magn. Magn. Mater.* **300** 127 (2006); cond-mat/0403641
21. Silov A Yu et al. *Appl. Phys. Lett.* **85** 5929 (2004)
22. Sih V et al. *Nature Phys.* **1** 31 (2005)
23. Golub L E, Ivchenko E L *Phys. Rev. B* **84** 115303 (2011)
24. Glazov M M, Sherman E Ya, Dugaev V K *Physica E* **42** 2157 (2010)

PACS numbers: 47.27.Gs, 47.35.Pq, 68.03.Kn
DOI: 10.3367/UFNe.0182.201208i.0879

Kinetic and discrete turbulence on the surface of quantum liquids

L V Abdurakhimov, M Yu Brazhnikov, A A Levchenko, I A Remizov, S V Filatov

1. Introduction

Wave turbulence is a nonequilibrium state in a system of interacting nonlinear waves in which the energy pumping and dissipation ranges are well separated in the wave number space. A turbulent state is characterized by a directed energy flux P in the k-space. Wave turbulence states can be realized in many nonlinear systems, for example, in plasmas [1], magnetic systems in solids [2], and on the surface of seas and oceans [3]. In our experiments, we explore the turbulence in a system of capillary waves, where surface tension plays the main role. Waves on a water surface are conventionally referred to as gravity waves if their wavelength exceeds 17 mm, and as capillary waves otherwise.

The frequency ω of capillary waves on the surface of a liquid is defined by the modulus of the wave vector k together with the surface tension coefficient σ and fluid density ρ:

$$\omega = \left(\frac{\sigma}{\rho}\right)^{1/2} k^{3/2} . \qquad (1)$$

Dispersion law (1) for capillary waves is of a decaying type, i.e., it permits the three-wave processes of wave decay into two waves or coalescence of two waves into a single wave while such that the energy and momentum are conserved,

$$\omega_1 \pm \omega_2 = \omega_3 , \qquad k_1 \pm k_2 = k_3 . \qquad (2)$$

When the surface of a liquid is excited by an external force, a turbulent state can develop in the system of capillary waves, in which the energy flux P in the k-space is directed from the pumping range toward large wave numbers (high frequencies), forming a direct cascade. Under the assumption that wave interactions are weak and hence the main contribution to energy transfer comes from three-wave processes, the theory of (weak) wave turbulence [4] predicts a power law for the energy distribution over frequencies, $E(\omega) \sim \omega^{-3/2}$.

However, exploring the energy frequency spectrum in experiments with capillary waves is a rather difficult task. From the standpoint of an experimentalist, it is most convenient to explore not the energy distribution E_ω but the pair correlation function $I(\tau) = \langle \eta(r, t+\tau)\, \eta(r, t) \rangle$ for the deviation of the surface elevation from equilibrium at a point r, because the deviation $\eta(r, t)$ from a planar surface is directly measurable.

The wave turbulence theory [4] for a system of capillary waves on the surface of a liquid predicts the formation of a turbulent cascade in the inertial range bounded by the pumping at low frequencies and the dissipation range at high frequencies. Within the inertial range, the pair correlation function $I(\tau)$ in the Fourier representation is described by a power-law function of the frequency (turbulent cascade):

$$I_\omega \sim \omega^{-m} , \qquad (3)$$

and $E(\omega) \sim \omega^{4/3} I_\omega$. The exponent m depends on the spectral characteristics of the driving force. Under the excitation of the surface of the liquid by a low-frequency noise in a broad band $\Delta\omega$ (with a bandwidth exceeding the characteristic pumping frequency ω_p, $\Delta\omega \geqslant \omega_p$), the turbulent cascade I_ω is described by the function ω^{-m} with the exponent $m = 17/6$. Numerical simulations [5] provide an estimate of m that is close to the theoretical prediction. The results of numerical modeling in Ref. [6] indicate that as the bandwidth of noise pumping $\Delta\omega$ is reduced, a series of equidistant peaks emerges in the turbulent cascade, with their widths behaving as a linear function of the frequency. For a narrow-band pumping, $\Delta\omega < \omega_p$, the decrease in the height of these peaks as the frequency increases is described by a power-law function of frequency with an exponent that exceeds the value for broadband noise pumping by one, i.e., $m = 23/6$.

Our experimental studies on the surface of liquid hydrogen have shown that the spectral characteristic of the applied force determines the value of the power-law exponent [7]. When the surface is perturbed by a low-frequency harmonic force, the correlation function I_ω exhibits a set of narrow peaks whose frequencies are multiples of the pumping frequency ω_p. The peak maxima are well described by a power law ω^{-m} with $m = 3.7 \pm 0.3$. When, in addition to pumping at a single resonance frequency, a harmonic force at another resonance frequency is applied, the exponent decreases to $m = 2.8 \pm 0.2$. The exponent was also close to $m = 3 \pm 0.3$ when the surface was excited by a broadband low-frequency noise. In these experiments, we have qualitatively shown that in passing from the surface excitation with broadband noise to pumping by a harmonic force at the single-cell resonance frequency, the exponent m increases. Detailed results characterizing the evolution of a turbulent

L V Abdurakhimov, M Yu Brazhnikov, A A Levchenko, I A Remizov, S V Filatov Institute of Solid State Physics, Russian Academy of Sciences, Chernogolovka, Moscow region, Russian Federation
E-mail: levch@issp.ac.ru

Uspekhi Fizicheskikh Nauk **182** (8) 879 – 887 (2012)
DOI: 10.3367/UFNr.0182.201208i.0879
Translated by S D Danilov; edited by A M Semikhatov

cascade under variations in the spectral characteristic of the excitation force (in passing from broadband pumping to a narrowband one) are obtained in Ref. [8].

In a stationary turbulent spectrum in a system of capillary waves, the energy is transferred to the region of high frequencies, where it is converted to heat through viscous losses, and the turbulent cascade decays. To keep the turbulent cascade in a stationary state, the energy has to be permanently supplied at low frequencies. The high-frequency boundary of the inertial range can be estimated by assuming that at the bounding frequency ω_b, the time scale of nonlinear wave interaction τ_{nl} becomes comparable in the order of magnitude to the viscous dissipation time τ_v [3],

$$\omega_b \sim \left(\frac{P^{1/2}}{\nu}\right)^{6/5} \sim \left(\frac{\eta_0^2\,\omega_0^{17/6}}{\nu}\right)^{6/5}, \quad (4)$$

where η_0^2 is the wave amplitude squared at the pumping frequency ω_p and ν is the kinematic viscosity of the liquid.

At high frequencies, the spectrum behavior is determined by the details of energy dissipation and nonlinear wave interaction. When waves in the dissipation range interact mainly with the nearest neighbors but not with waves from the inertial range, the wave distribution at high frequencies becomes close to exponential [9]. A detailed analysis [10] gives a quasi-Planck spectrum for the correlation function in the dissipation range,

$$P_\omega \sim \omega^s \exp\left(-\frac{\omega}{\omega_d}\right), \quad (5)$$

where ω_d is the characteristic frequency of the distribution. Results of numerical modeling for capillary waves [10] corroborated the exponential dependence of the wave distribution in the dissipative range. In our research, we therefore concentrated on a detailed study of the evolution of a turbulent cascade as the bandwidth $\Delta\omega$ was varied: from broadband noise pumping (kinetic regime) to narrow-band noise excitation, and further to monochromatic pumping (discrete mode).

In bounded geometries, the continuous spectrum of capillary waves becomes discrete, whereas the separation between the resonance modes increases with the frequency. In the case of monochromatic forcing of the liquid surface, the turbulent cascade consists of harmonics whose frequencies are multiples of the pumping frequency. Simple reasoning leads to the conclusion that for such surface excitation, system of equations (2) does not have any solutions [11, 12]. However, as shown in Ref. [13], this limitation is lifted if nonlinear broadening of resonance peaks is taken into account. In that case, the conservation laws have to be written as

$$\left||k_1|^{3/2} \pm |k_2|^{3/2} - |k_3|^{3/2}\right| < \delta, \qquad k_1 \pm k_2 - k_3 = 0, \quad (6)$$

where δ is the characteristic nonlinear broadening of the resonance peak. Additionally, it is necessary to take into account that for a classical liquid at high frequencies, the discrete spectrum becomes quasicontinuous because of viscous broadening of the resonance peaks. But in liquid hydrogen and, especially, helium, the kinematic viscosity coefficient is less than in water, by a factor of 10 for hydrogen and 100 for helium. Therefore, the quantization can play an important role in the energy transfer in the cascade [14] under monochromatic excitation. Our work [15] presents results obtained on the surface of superfluid helium under harmonic forcing when the discrete character of the system is essential (discrete turbulence). At the same time, for broadband pumping applied to surfaces of liquid hydrogen and helium, the case of kinetic turbulence is realized, which is closest to the model system worked out theoretically in Ref. [4].

2. Experimental procedure

In recent years, owing to advances in experimental technology and computer methods for processing rapidly varying signals, substantial progress has been achieved in exploring capillary turbulence on the surface of water [16–19], ethanol [20], silicon oil [21], and even mercury [22]. Our previous experiments [23] have shown that using liquid helium and hydrogen in studies of turbulence offers a number of advantages over the use of traditional media owing to the small density and low kinematic viscosity of helium and hydrogen.

In our research, we used a technique [24] based on measuring the power of a laser beam reflected from the oscillating surface of a liquid. Measurements were conducted in optical cells located in the vacuum cavity of a helium cryostat. A plane horizontal capacitor was installed inside the cells. Gaseous hydrogen or helium was condensed in a cylindrical copper cup. Its diameter was 60 mm in experiments with hydrogen and 30 mm in experiments with helium. The cup height was varied in the range 4–6 mm. Above the cup, the upper horizontal metallic plate of a capacitor was mounted, leaving a gap of 3.5 mm. The liquid was accumulated until it reached the edge of the cup. The temperature during measurement was $T = 15.5$ K in experiments with hydrogen and 1.7 K in experiments with helium.

The lower plate of the capacitor is fitted with a radioactive source emitting β-electrons with the mean energy 5 keV. Under the action of radiation, an ionized layer of liquid is formed in the vicinity of the source. A voltage of 1000 V applied to the capacitor plates drives positive ions out of the ionized layer toward the surface of the liquid. In this manner, the charged liquid surface and the upper metallic plate form a plane capacitor.

Waves on the charged fluid surface are excited by an alternating electric field generated by AC voltage with an amplitude of 1–100 V applied to the metallic cup, in addition to DC voltage. Pumping either is harmonic at frequencies close to the resonant frequencies of the cylindrical cell or represents broadband noise. The noise pumping signal was synthesized through the inverse Fourier transformation given the power spectrum and applying random phases. Using an electric field to excite the surface of the liquid offers a number of advantages. Indeed, it allows applying the force only to the surface and controlling the symmetry of forcing together with its spectral characteristics.

Changes in the power of the reflected laser beam were measured by a Hamamatsu s3590-08 semiconductor receiver. The AC output of the photoreceiver $P(t)$, proportional to the power of the reflected ray, was stored in computer memory at a sampling rate up to 100 kHz with the help of a fast 24-bit analog-to-digital converter (ADC). The recording time of the signal $P(t)$ was varied from 3 s to 100 s. The dependences $P(t)$ were processed with a fast Fourier transform (FFT) routine. As a result, we obtained the distribution of the squared amplitude of the harmonics over frequency P_ω^2, which for a

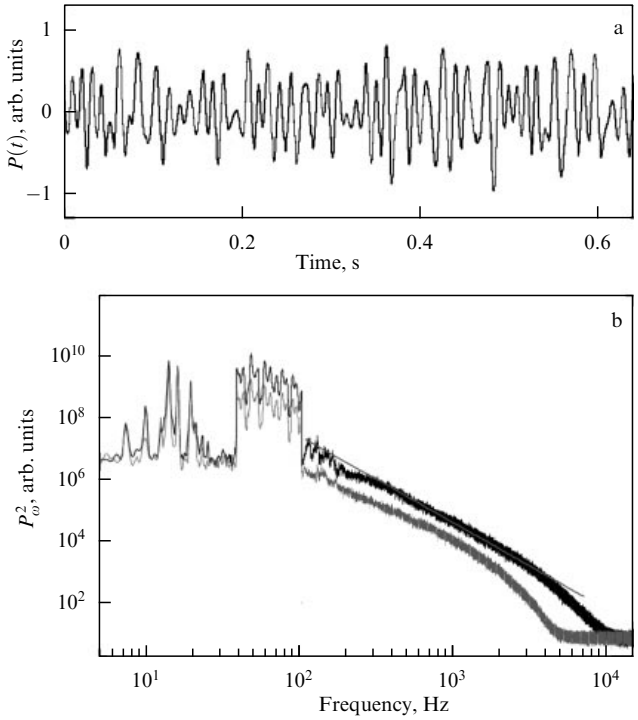

Figure 1. (a) Part of the experimental record of $P(t)$. Pumping is carried out with a random force in the frequency range 39–103 Hz. (b) Turbulent cascade on the surface of liquid hydrogen excited by a random force in the frequency range 39–103 Hz for two pumping levels. The straight line is the dependence $\omega^{-17/6}$.

broad beam, as shown in Ref. [24], is proportional to the pair correlation function for the surface deviation from equilibrium, $I_\omega \sim P_\omega^2$.

3. Modification of a turbulent cascade with a reduction in the forcing bandwidth

Figure 1a shows part of the signal $P(t)$ recorded from the surface of liquid hydrogen excited by noise. The bandwidth of the electric signal $V(t)$ applied to the guard ring was 64 Hz (from 39 Hz to 103 Hz), i.e., the surface was excited by broadband noise. The maximum amplitude of the noise forcing signal was 10 V, while maximum steepness of waves (angular amplitude) did not exceed 0.03 in the pumping range.

Figure 1b shows the distribution P_ω^2 (the dark curve) that corresponds to the signal in Fig. 1a. In the frequency range from 200 Hz to 8 kHz, a turbulent cascade formed whose frequency dependence was described by a power law with the exponent $m = 2.8 \pm 0.1$. For comparison, the straight line shows a function proportional to $\omega^{-17/6}$. The deviation from the power law at high frequencies (4–8 kHz) is a manifestation of the impact of viscous losses in the liquid on the turbulent distribution [4]. The dissipation range becomes well pronounced as the excitation force amplitude decreases. The light curve in Fig. 1b corresponds to the spectrum P_ω^2 with pumping in the same frequency range, but with the amplitude two and half times smaller. The high-frequency boundary of the inertial range decreased to 2.5 kHz. In the frequency range above 2.5 kHz, a sharp reduction in the oscillation amplitude is observed, which is characteristic of the spectrum in the dissipation range.

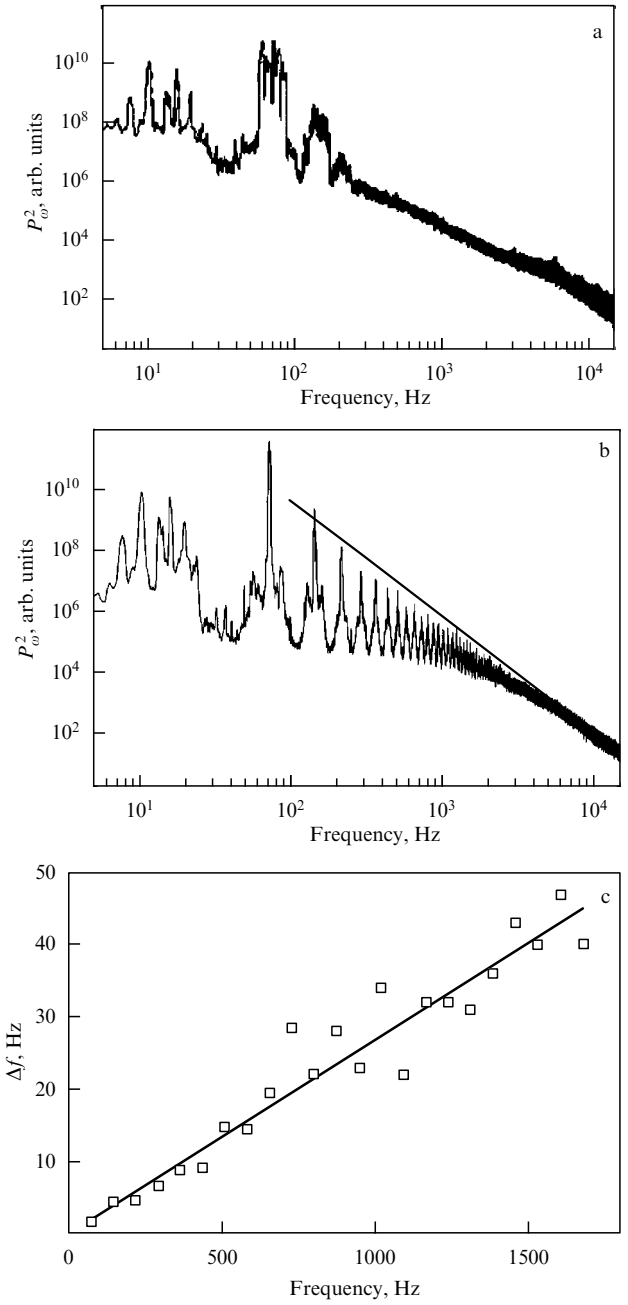

Figure 2. (a) The spectrum P_ω^2 of surface oscillations forced by noise in the frequency range 57–89 Hz. (b) The same as (a), but in the frequency range 71–75 Hz. The straight line corresponds to the dependence $\omega^{-23/6}$. (c) The dependence of the peak width Δf in the spectrum of panel (a) on frequency. The straight line is the linear law 0.027ω.

When the bandwidth of noise pumping was reduced relative to the mean pumping frequency such that $\Delta\omega \approx \omega/2$, several peaks emerged on the turbulent cascade. The distribution P_ω^2 for noise pumping in the frequency range 57–89 Hz is shown in Fig. 2a. The angular wave amplitude was 0.03, the same as in the previous case. The first peak lies in the pumping range. The second and third peaks correspond to waves appearing as a result of a nonlinear interaction. The separation between the centers of the peaks is approximately equal to the pumping frequency $\omega_p = 73$ Hz. It is clearly seen that a well-developed turbulent cascade formed in the frequency range 250 Hz–6 kHz. At frequencies above the

upper boundary of the inertial range $\omega_b = 6$ kHz, the decay of the cascade is observed, caused by viscous losses.

As the pumping bandwidth $\Delta\omega$ is reduced further, the peaks in the turbulent cascade become more expressed, and the minima go deeper. Figure 2b shows the distribution P_ω^2 when the surface is excited by noise in the frequency band of 4 Hz (from 71 Hz to 75 Hz). About 30 peaks are distinctly visible in the turbulent cascade. The separations between the peaks stays the same (73 Hz). The inertial range extends from 200 Hz to 15 kHz. The frequency dependence of peak maxima within the inertial range is close to the power law $\omega^{-3.8\pm0.1}$. We note that the difference in exponents in cases of narrow- and broadband pumping is 1.0 ± 0.2.

The peak widths Δf increase with frequency. The experimental dependence of peak widths on frequency is presented in Fig. 2c for noise pumping in the frequency range 71–75 Hz. Obviously, the increase in Δf with frequency is described by a linear function, and satisfactory agreement is observed between experimental data and the linear dependence predicted by the theory. The solid line in Fig. 2c corresponds to the linear function $\Delta f = 0.027\omega$. This means that the effective width of the pumping range in the capillary wave system is about 2 Hz, while the noise bandwidth in the electric signal applied to the guard ring is 4 Hz. This discrepancy comes from the discreteness of the capillary wave spectrum in the experimental cell and the finite width of resonance modes. The separation between two neighboring resonances at frequencies about 100 Hz amounts to ≈ 10 Hz for the peak width about 1 Hz. Thus, for a surface forced with noise in the frequency band of 4 Hz, there is such a position of the pumping interval relative to the resonance frequencies of the cell that only a single resonance harmonic can be excited. Arguably, this happens in the case displayed in Fig. 2b.

The linear dependence of the peak width on frequency can readily be explained [6]. Indeed, if nonlinear waves are excited in the range $\omega_p \pm \Delta\omega$, then, by virtue of the nonlinear interaction between them, waves appear in the frequency range $2\omega_p \pm 2\Delta\omega$, and so on. Hence, the linear dependence of the peak width on frequency must pass through the coordinate origin. Precisely these considerations have been used to draw the solid line in Fig. 2c.

The experimental results presented above showed that the change in the spectral characteristics of noise forcing (the bandwidth) leads to a qualitative modification of the turbulent cascade in the system of capillary waves on the surface of liquid hydrogen. For broadband pumping, the turbulent distribution is described well by a monotonically decaying power-law function with the exponent close to $m = 2.8 \pm 0.1$. By contrast, for narrowband forcing, a set of peaks appears in the turbulent cascade, their maxima following the power law with the exponent $m = 3.8 \pm 0.1$. Our results turn out to be in very good agreement with theory.

4. The decay of the turbulent cascade in the dissipation range

In the same fashion as in the experiments described in Section 3, capillary waves on the surface of liquid hydrogen were excited by a random force in the range 39–103 Hz. The mean amplitude of AC voltage (pumping) V_p, averaged over the frequency range, was varied from zero (in the absence of pumping) to the maximum amplitude $V_p = 30$ V, which was limited by the maximum angular wave amplitude allowed by the geometry of our low-temperature optical system.

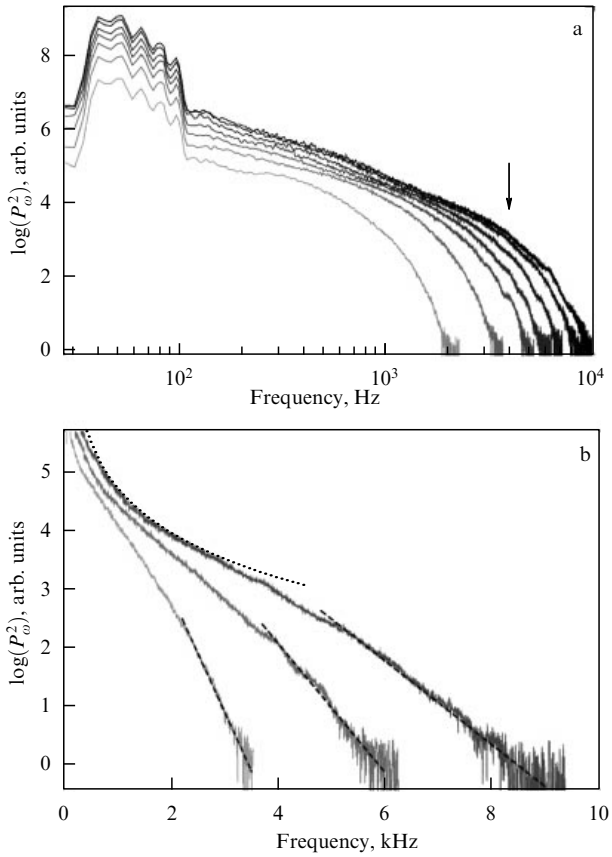

Figure 3. (a) The spectrum of surface oscillations P_ω^2 excited by a random force in the frequency range 39–103 Hz with different pumping amplitudes. The pumping amplitude is varied from 4 V (light curve) to 30 V (dark curve). The arrow marks the high-frequency boundary of the inertial range for maximum pumping. (b) The spectra P_ω^2 obtained for pumping with amplitudes $V_p = 8$, 16, and 26 V. The dotted line corresponds to the power law $\omega^{-2.8}$. The dashed lines represent the approximation by the function $\sim \exp(-\omega/\omega_d)$ with $\omega_d \approx 0.2$, 0.4, and 0.6 kHz for $V_p = 8$, 16, and 26 V, respectively.

Figure 3a shows the Fourier spectrum of the power of a reflected laser beam for various excitation amplitudes. The pumping range can well be discerned on the low-frequency side. It is followed by the inertial range within which the spectrum P_ω^2 can be described by power law (3). The width of the inertial range, as is clearly seen, depends on the pumping amplitude. When the surface is excited with a force that corresponds to the amplitude $V_p = 4$ V, the dissipative range begins immediately after the pumping range, while the inertial range is absent. The increase in the amplitude of the driving force expands the inertial range, and its high-frequency boundary ω_b shifts toward higher frequencies. The widest inertial range, from 0.3 to 4 kHz, is observed for the maximal pumping amplitude $V_p = 30$ V. At frequencies above the inertial range boundary, surface perturbations decay because of viscous losses, and the cascade smoothly fades out, disappearing in instrumental noise. The turbulent cascades recast in linear coordinates (Fig. 3b) show that the decay in the wave amplitude in the dissipative range can be approximated rather well by the exponential dependence $P_\omega^2 \sim \exp(-\omega/\omega_d)$. In the fitting, it is assumed that $\omega \gg \omega_d$, i.e., that the characteristic frequency (viscous boundary) ω_d is much lower than the frequency of waves from the dissipation range. For example, the spectrum obtained for pumping with the amplitude $V_p = 26$ V is approximated by the exponential

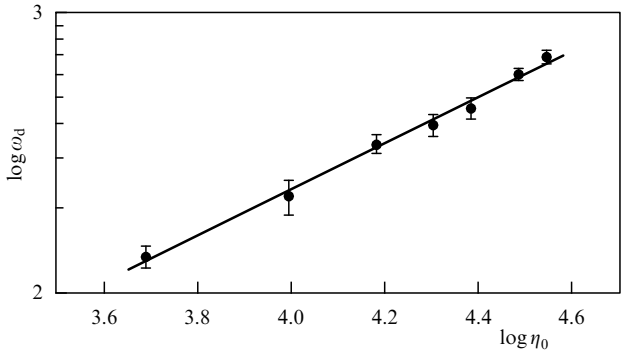

Figure 4. The dependence of the frequency ω_d on the amplitude of low-frequency pumping η_0; the straight line is the fit $\eta_0^{0.85}$.

with $\omega_d = 0.6$ kHz in the frequency range 5–9 kHz. Unfortunately, the fitting interval turns out to be insufficiently broad for reliably estimating the power of the pre-exponential factor in quasi-Planck distribution (5). The values of ω_d thus found are several times smaller than the visible boundaries separating the inertial range and dissipation range (Fig. 3b). This discrepancy can be explained by some arbitrariness in the definition of the high-frequency inertial range boundary, and hence the value of ω_b is only known by an order of magnitude. The characteristic frequency ω_d obtained by fitting an exponential to the spectra grows with the pumping amplitude in the dissipation range. To correctly plot the dependence of ω_d on the pumping amplitude, we used the surface response $\eta_0 = P$ at the frequency 53 Hz as a measure of the excitation level. The quantity η_0 is directly proportional to the mean wave amplitude at this frequency. Figure 4 shows the dependence of ω_d on the amplitude η_0. The experimental dependence is described by the power law $\omega_d(\eta_0) \sim \eta_0^n$ with the exponent $n = 0.85 \pm 0.05$.

It is noteworthy that the approximation of experimental spectra with quasi-Planck distribution with a small value of the exponent s (no higher than 2) does not significantly affect the value of ω_d (by less than 20%), nor does it influence the power-law exponent n in the amplitude dependence of the characteristic frequency $\omega_d(\eta_0)$.

The obtained value of the exponent $n = 0.85$ differs substantially from the value 12/5 expected from Eqn (4), which is surprising because for a turbulent cascade formed by a harmonic force, the measured amplitude dependence proves to be in good agreement with the theoretical estimate $\omega_d(\eta) \sim \eta^{1.3}$.

We note especially that the turbulent cascade in the dissipation range decays noticeably faster for monochromatic than for broadband pumping. Figure 5a shows the turbulent cascade at the surface of superfluid helium forced monochromatically at a frequency of 79.7 Hz. The turbulent cascade very closely resembles distributions observed previously in experiments on the surface of liquid hydrogen [7] and in our first studies on the superfluid helium surface [25]. The spectrum consist of equidistant harmonics: the first harmonic corresponds to pumping, while the others are generated as a result of the nonlinear interaction of waves with frequencies that are multiples of the pumping frequency. At frequencies greater than 4 kHz, the cascade decays extremely rapidly because of viscous losses and disappears, being buried in instrumental noise. The value of 4 kHz can be treated as the high-frequency boundary ω_b of the inertial range. The decay is described by an exponential dependence with the characteristic frequency $\omega_d = 170$ Hz close to the

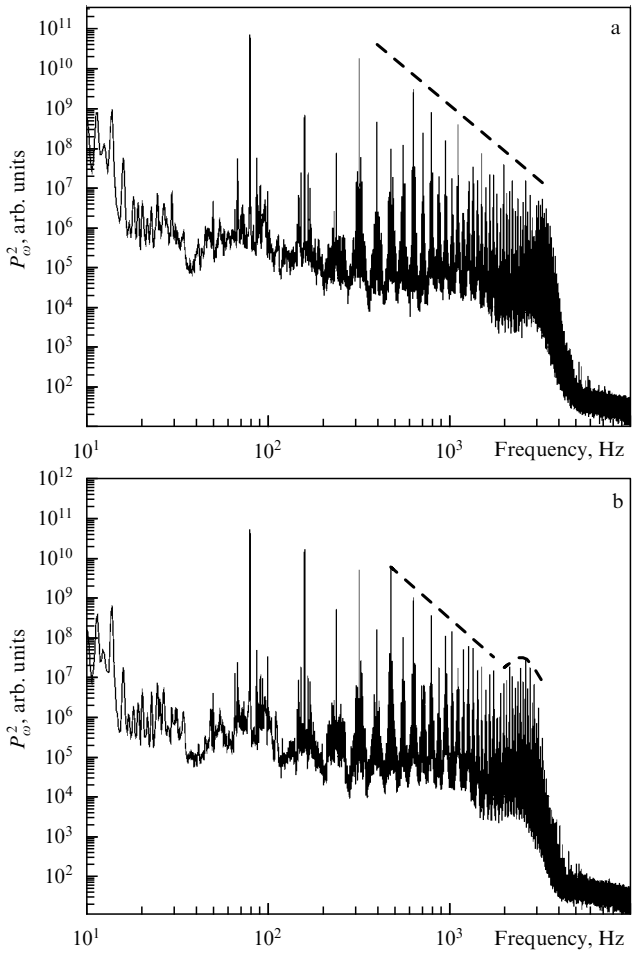

Figure 5. (a) The distribution P_ω^2 on the surface of superfluid helium at the temperature 1.7 K. The surface was excited by a sinusoidal force at a frequency of 79.7 Hz. The pumping amplitude was 11 V. The dashed line corresponds to the power law $P_\omega^2 \sim \omega^{-3.7}$ theoretically predicted for random narrowband pumping. (b) Turbulent spectrum as the amplitude of forcing is reduced to 10 V. A local maximum is observed near the frequency 2.5 kHz (marked by the dashed line).

pumping frequency ω_p [26]. We mention that for broadband forcing of the superfluid helium surface, the turbulent distribution in the dissipation range smoothly decays following an exponential law with the characteristic frequency ω_b that is close to the frequency of the high-frequency edge of the inertial range (Fig. 6b).

We can assume that the condition of locality for waves from the dissipation range is violated under harmonic excitation. For these waves, the interaction with waves from the inertial range proves to be dominating. Indeed, the nonlinear interaction time for three-wave processes with strongly different wave vectors ($k_1 \ll k_2$, $k_2 \approx k_3$) satisfies the relationship $\tau_{non} \sim k^{-1/2}$ [10], whereas for the local interaction ($k_1 \approx k_2 \approx k_3$) the time $\tau_{loc} \sim k^{1/4}$ [27]. Thus, the waves from the dissipation interval most efficiently interact with low-frequency waves from the inertial range, concentrated in the vicinity of the pumping range.

5. Discrete turbulence

In experimental studies of turbulent distributions on the surface of superfluid helium, we used two types of driving forces to generate surface waves. In experiments of the first type, the surface was excited by a sinusoidal force at one of the

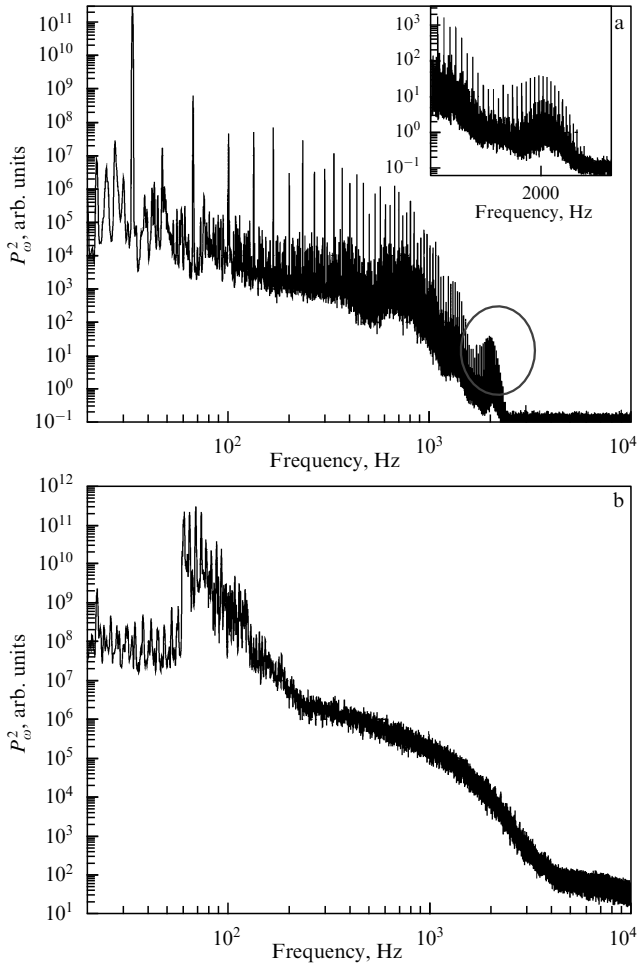

Figure 6. (a) Turbulent spectrum for pumping at the frequency $\omega/2\pi = 34$ Hz. The local maximum in the dissipation range is zoomed in in the inset. (b) The turbulent cascade of capillary waves pumped with noise in the frequency range 60–130 Hz.

cell resonance frequencies. In experiments of the second type, the surface was excited by noise in a bounded frequency range.

Figure 5a displays the spectrum P_ω^2 of capillary waves obtained in an experiment in which the superfluid helium surface was forced by an AC voltage at the frequency 79.7 Hz and amplitude 11 V. In the inertial range, the amplitudes of the harmonics decay with frequency according to the power law $P_\omega^2 \sim \omega^{-m}$ with $m \approx 3.7$, in agreement with the theoretical prediction for narrowband forcing [6].

If the forcing amplitude is slightly reduced, to 10 V, the shape of the turbulent cascade experiences qualitative changes. The high-frequency boundary of the inertial range shifts toward low frequencies, in agreement with the results of our previous experiments [7]. However, a new phenomenon is observed: the formation of a distinct local maximum close to the high-frequency boundary ω_b of the inertial range (marked by the dashed line in Fig. 5b). As the pumping amplitude is reduced further, the local maximum shifts to low frequencies. The spectrum consist of several harmonics for minimum pumping, and the local maximum is not observed.

We summarize common features of the results obtained in experiments. First, a local maximum is formed at high frequencies close to the end of the inertial range. Second, the shape and position of the maximum depend on the pumping frequency ω_p and the pumping wave amplitude. For example, Fig. 6a shows the spectrum P_ω^2 obtained for the surface of helium forced sinusoidally at a frequency of 34 Hz, with a well-pronounced maximum in the dissipation range, and not in the inertial range as in Fig. 5b.

When the surface is forced by noise, the local maximum is not observed. As an illustration, Fig. 6b presents a turbulent distribution for a helium surface forced with noise in the frequency range 60–130 Hz. The pumping amplitude was selected such that the end of the inertial range was located at the same frequencies as in Fig. 5b. It can be seen that this spectrum is qualitatively different from spectra obtained with monochromatic pumping: it is smooth and continuous.

The formation of a local maximum can be interpreted as energy accumulation in a narrow frequency interval near the end of the inertial range where the transition from nonlinear energy transfer to viscous decay occurs. A possible reason for this accumulation can be a bottleneck that impedes energy transfer to the dissipation range. It was shown in [10] that an insufficient rate of energy dissipation through viscous losses can in principle essentially modify the cascade shape at high frequencies in the inertial range. However, judging by the frequency and amplitude dependences of the maximum position, the formation of the cascade is not related to the trivial influence of viscosity. On the other hand, we are dealing with a weakly interacting nonlinear discrete wave system, and, as shown in Refs [11, 12], we can expect the discreteness of the system to affect wave interactions. In the later study [13], a model of frozen turbulence was proposed, and it was shown that the discreteness can result in an oscillating turbulent spectrum for surface waves in a square geometry, when the wave number space is two-dimensional. In our experiment, the geometry is circular, surface oscillations are described by the Bessel functions, and the wave number space is one-dimensional. Because the cell shape and size define the density of resonance modes, we made some estimates in order to understand the influence of the discrete character of spectra on the turbulent cascade in our experiments. We suppose that the main reason for the bottleneck and, consequently, the maximum formation is a detuning between frequencies of two discrete spectra, namely the spectrum of surface oscillations in a finite-size cell and the spectrum of turbulent cascade harmonics. If the surface is excited by a harmonic force, the frequency of the first peak in the turbulent cascade coincides with the frequency of resonance harmonics ω_p, which satisfies dispersion relation (1).

For surface waves in a cylindrical cell of diameter D, the resonance values of wave vectors satisfy the equation $J_1(kD/2) = 0$, where $J_1(x)$ is the Bessel function of the first order. For large magnitudes of wave vector k, the resonances becomes equidistant with the step $\Delta k \approx 2\pi/D$. Consequently, the distance between two nearest resonances in the frequency space increases with frequency:

$$\Delta\omega = \frac{\delta\omega}{\delta k}\,\Delta k \approx 2\pi\,\frac{\delta\omega}{\delta k}\,\frac{1}{D} = \frac{3\pi}{D}\left(\frac{\sigma}{\rho}\right)^{1/3}\omega^{1/3}. \qquad (7)$$

In other words, resonances in the case of capillary waves are not equidistant, in contrast to frequencies of harmonics in the turbulent cascade, which are multiples of the pumping frequency ω_p.

Obviously, frequency detuning can be essential only when the resonance broadening $\delta\omega$ is small compared to the

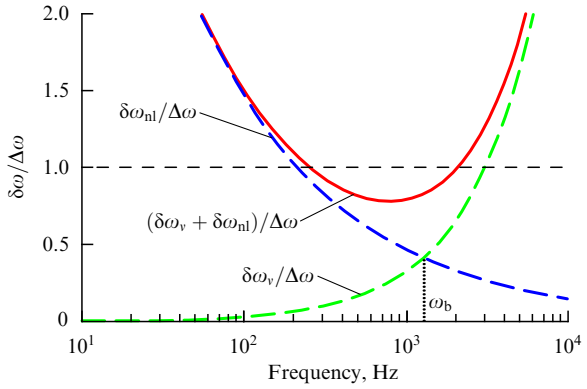

Figure 7. The estimate of the relative broadening $\delta\omega/\Delta\omega$ for harmonic pumping of moderate amplitude. The increasing dashed curve represents the relative viscous broadening $\delta\omega_v/\Delta\omega$, the decreasing dashed curve depicts the relative nonlinear broadening $\delta\omega_{\rm nl}/\Delta\omega$, and the solid curve with a minimum corresponds to the total relative broadening $\delta\omega/\Delta\omega$.

separation between resonances $\Delta\omega$ (Fig. 7),

$$\frac{\delta\omega}{\Delta\omega} < 1\,. \tag{8}$$

The resonance broadening $\delta\omega$ can be represented as a sum of viscous $\delta\omega_v$ and nonlinear $\delta\omega_{\rm nl}$ broadening:

$$\delta\omega = \delta\omega_v + \delta\omega_{\rm nl}\,. \tag{9}$$

Broadening of the resonance peak caused by viscous losses increases with the frequency,

$$\delta\omega_v = 4\nu\kappa_\omega^2 = 4\nu\left(\frac{\rho}{\sigma}\right)^{2/3}\omega^{4/3}\,, \tag{10}$$

while the characteristic time of viscous damping decreases, $\delta\omega_v = \tau_v^{-1}$.

Broadening due to the nonlinear energy transfer in the turbulent cascade can be estimated from the characteristic time of nonlinear interaction $\tau_{\rm nl}$ as $\delta\omega_{\rm nl} = \tau_{\rm nl}^{-1}$. In the case of harmonic pumping, we assume that $\tau_{\rm nl} \sim \omega^{1/6}$ [7], whence $\delta\omega_{\rm nl} \sim \omega^{-1/6}$. As the driving force amplitude A increases, the nonlinearity of waves increases, if the frequency is kept fixed. We can therefore write

$$\delta\omega_{\rm nl} \approx \varepsilon(A)\,\omega^{-1/6}, \tag{11}$$

where $\varepsilon(A)$ is an increasing function of the wave amplitude A at the pumping frequency. Substituting Eqns (7) and (9)–(11) in Eqn (8), we obtain the condition for the detuning to be important:

$$\frac{4\nu(\rho/\sigma)^{2/3}\omega^{4/3} + \varepsilon(A)\,\omega^{-1/6}}{(3\pi/D)(\sigma/\rho)^{1/3}\omega^{1/3}} < 1\,.$$

On the high-frequency boundary $\omega_{\rm b}$ of the inertial range, the nonlinear energy transfer along the spectrum gives way to viscous dissipation. Therefore, as noted above, it is assumed that at the frequency $\omega_{\rm b}$, the characteristic time of viscous damping is close to that of nonlinear interaction, $\tau_v(\omega_{\rm b}) \approx \tau_{\rm nl}(\omega_{\rm b})$. Although the precise form of the function $\varepsilon(A)$ is unknown, we can conclude that the resonance peak broadenings induced by the nonlinear interaction and by viscous losses are also close to each other at the frequency $\omega_{\rm b}$, $\delta\omega_v(\omega_{\rm b}) \approx \delta\omega_{\rm nl}(\omega_{\rm b})$.

It follows from estimates that in our experiments, the total relative broadening of the resonance peak satisfies condition (8) in a finite frequency interval located near the high-frequency boundary $\omega_{\rm b}$ (see Fig. 7). In this interval, the frequency detuning between harmonics in the turbulent cascade and resonance peaks becomes essential, and the discrete regime of capillary turbulence is realized. Following the logic of Ref. [10], we suppose that the energy flux bottleneck forms in that region, which determines the specific shape of the distribution P_ω^2. At high pumping amplitudes (or at high frequencies), the relative broadening exceeds unity, the system becomes quasicontinuous, and the kinetic regime of turbulence is realized. However, based on this simple assumption, we cannot compute the exact position of the local maximum or its form. Rigorous theoretical analysis and numerical simulations are needed.

The proposed model presumes that the following conditions, needed for the energy to accumulate in a system of capillary waves, are satisfied: insignificant viscous broadening of the resonance peak, not very strong nonlinear broadening (moderate pumping amplitudes), and large separation between neighboring resonance frequencies (a relatively small cell size). We stress that it is the use of superfluid helium with extremely low viscosity [28] that enabled us to observe the energy condensation in the turbulent cascade.

6. Conclusions

Passing from broadband to narrowband and further to harmonic pumping in experiments on the formation of a turbulent state in a system of capillary waves leads to a qualitative change in the turbulent distribution: a set of peaks evolves in the cascade modifying the frequency dependence of the correlation function. A quasi-Planck distribution of waves over frequency is formed in the dissipation range with the characteristic frequency defined by spectral characteristics of pumping.

Using superfluid helium with an extremely low value of kinematic viscosity enabled observing the discrete regime of capillary turbulence. The influence of the discreteness of the surface oscillation spectrum on the turbulent distribution is manifested in the formation of a local maximum near the end of the inertial range — the energy condensation in a narrow frequency range. The fundamental cause of this phenomenon is the frequency detuning between the harmonics in the turbulent cascade and resonance modes of the cylindrical resonator, and also in the formation of a bottleneck for the energy flux toward higher frequencies.

The authors are grateful to L P Mezhov-Deglin, E A Kuznetsov, and G V Kolmakov for the useful discussions. The research was supported in part by the RFBR grant 11-02-12147.

References

1. Musher S L, Rubenchik A M, Zakharov V E *Phys. Rep.* **252** 177 (1995)
2. L'vov V S *Wave Turbulence under Parametric Excitation: Applications to Magnets* (Berlin: Springer-Verlag, 1994)
3. Zakharov V E, Filonenko N N *Zh. Priklad. Mekh. Tekh. Fiz.* **8** 37 (1967) [*J. Appl. Mech. Tech. Phys.* **8** 62 (1967)]
4. Zakharov V E, L'vov V S, Falkovich G *Kolmogorov Spectra of Turbulence* Vol. 1 (Berlin: Springer-Verlag, 1992)
5. Pushkarev A N, Zakharov V E *Phys. Rev. Lett.* **76** 3320 (1996)

6. Fal'kovich G E, Shafarenko A B *Zh. Eksp. Teor. Fiz.* **94** 172 (1988) [*Sov. Phys. JETP* **67** 1393 (1988)]
7. Brazhnikov M Yu, Kolmakov G V, Levchenko A A *Zh. Eksp. Teor. Fiz.* **122** 521 (2002) [*JETP* **95** 447 (2002)]
8. Abdurakhimov L V, Brazhnikov M Yu, Levchenko A A *Pis'ma Zh. Eksp. Teor. Fiz.* **89** 139 (2009) [*JETP Lett.* **89** 120 (2009)]
9. Malkin V M *Zh. Eksp. Teor. Fiz.* **86** 1263 (1984) [*Sov. Phys. JETP* **59** 737 (1984)]
10. Ryzhenkova I V, Fal'kovich G E *Zh. Eksp. Teor. Fiz.* **98** 1931 (1990) [*Sov. Phys. JETP* **71** 1085 (1990)]
11. Kartashova E A *Physica D* **46** 43 (1990)
12. Kartashova E A *Physica D* **54** 125 (1991)
13. Pushkarev A N, Zakharov V E *Physica D* **135** 98 (2000)
14. Zakharov V E et al. *Pis'ma Zh. Eksp. Teor. Fiz.* **82** 544 (2005) [*JETP Lett.* **82** 487 (2005)]
15. Abdurakhimov L V, Brazhnikov M Yu, Remizov I A, Levchenko A A *Pis'ma Zh. Eksp. Teor. Fiz.* **91** 291 (2010) [*JETP Lett.* **9**1 271 (2010)]
16. Wright W B, Budakian R, Putterman S J *Phys. Rev. Lett.* **76** 4528 (1996)
17. Henry E, Alstrøm P, Levinsen M T *Europhys. Lett.* **52** 27 (2000)
18. Punzmann H, Shats M G, Xia H *Phys. Rev. Lett.* **103** 064502 (2009)
19. Brazhnikov M Yu, Kolmakov G V, Levchenko A A, Mezhov-Deglin L P *Europhys. Lett.* **58** 510 (2002)
20. Falcón C et al. *Europhys. Lett.* **86** 14002 (2009)
21. Westra M-T *Patterns and Weak Turbulence in Surface Waves* (Eindhoven: Technische Univ. Eindhoven, 2001)
22. Falcon É, Laroche C, Fauve S *Phys. Rev. Lett.* **98** 094503 (2007)
23. Kolmakov G V et al. *Prog. Low Temp. Phys.* **16** 305 (2009)
24. Brazhnikov M Yu, Levchenko A A, Mezhov-Deglin L P *Prib. Tekh. Eksp.* (6) 31 (2002) [*Instrum. Exp. Tech.* **45** 758 (2002)]
25. Abdurakhimov L V, Brazhnikov M Yu, Levchenko A A *Fiz. Nizk. Temp.* **35** 127 (2009) [*Low Temp. Phys.* **35** 95 (2009)
26. Abdurakhimov L V, Brazhnikov M Yu, Levchenko A A *J. Phys. Conf. Ser.* (2012), accepted
27. Kolmakov G V *Pis'ma Zh. Eksp. Teor. Fiz.* **83** 64 (2006) [*JETP Lett.* **83** 58 (2006)]
28. Donnelly R J, Barenghi C F *J. Phys. Chem. Ref. Data* **27** 1217 (1998)

PACS numbers: **95.75.–z**, **96.50.–e**, **96.60.–j**
DOI: 10.3367/UFNe.0182.201208j.0887

Motion of the Sun through the interstellar medium

V G Kurt, E N Mironova

1. Introduction

The motion of the Sun includes many components with different velocities, directions, and reference systems. For example, the Sun moves in a complicated open trajectory around the solar system barycenter. The maximum amplitude of this motion sometimes exceeds the radius of the Sun itself. This excursion is due to the motion of the most massive planets in the Solar System, Jupiter and Saturn, with the respective orbital periods 11.859 and 29.428 years. The Sun also moves relative to the 100 nearest stars in the direction toward the Hercules constellation with a velocity of 19.2 km s^{-1}. This motion was discovered by W Herschel (1738–1822) at the end of the 18th century based on the analysis of proper motions of the brightest (and correspondingly closest) stars. Naturally, Herschel could not express the value of this velocity in units such as km s^{-1} because he did not know the distance to these stars. Distances to stars were measured only in the early 1830s almost simultaneously by V Ya Struve (1793–1864) (Russia), F Bessel (1784–1846) (Prussia), and T Henderson (1798–1844) (England) using annual parallaxes of stars, which amount to only fractions of an arc second, even for the nearest stars. The direction to the apex of this motion is $\alpha = 270^\circ$ and $\delta = 30^\circ$.

The Sun also participates in an almost circular orbital motion around the galactic center with a velocity of 220 km s^{-1} in the direction perpendicular to the direction to the galactic center. With the distance 7.9 kpc to the galactic center, the orbital period of this motion is about 200 mln years, and during its life (5 billion years), the Sun has already made about 25 revolutions around the galactic center.

The Sun, together with the Galaxy, also has a peculiar velocity relative to nearby galaxies of the Local Group of galaxies. For example, the Galaxy approaches the center of the Andromeda nebula (M31) with a velocity of 290 km s^{-1} relative to the Solar System barycenter.

Finally, the Sun, together with the Milky Way and the Local Group, moves relative to the isotropic 3 K cosmic microwave background with the velocity (667 ± 22) km s^{-1} in the direction $l = 276^\circ \pm 3^\circ$ and $b = 30^\circ \pm 3^\circ$ (galactic coordinates). In a certain sense, this reference frame is a peculiar, singular coordinate system. Just this motion is responsible for the presence of the dipole component in the decomposition of cosmic microwave background in spherical functions. The amplitude of the dipole component is 6.706 mK.

This paper is focused on the study of the motion of the Sun relative to the local interstellar medium (LISM) on scales smaller than one or several parsecs but larger than 1000 astronomical units (a.u.).

2. Brief history of the discovery of the motion of the Sun relative to the local interstellar medium

In 1959, a group of astronomers from the Naval Research Laboratory (NRL) in the USA headed by G Fridman discovered a bright UV glowing of the sky from the rocket Aeroby-χ, which was capable of reaching only a 140 km altitude. The glow was measured in the atomic hydrogen line L_α ($\lambda = 1215.7$ Å) with the intensity reaching 20 kR (1 Rayleigh (R) = 10^6 photons cm^{-2} s^{-1} $(4\pi$ sr$)^{-1}$). The minimum of this glow was found to come from the anti-solar direction, and its intensity at a distance exceeding 90 km from Earth slowly decreased with increasing height [1]. In the same year, using a cell filled with molecular hydrogen supplied with a filament for its dissociation, which provided a sufficient amount of neutral hydrogen atoms for L_α line absorption, Morton determined that 7% of the discovered UV emission has a temperature exceeding 7000 K [2]. This could be explained by the presence of both a hot atomic hydrogen component in the upper atmosphere of Earth and an extra-atmosphere 'hot' emission component.

At almost the same time, starting in 1961, a research program of the Moon, Venus, and Mars explorations using automatic interplanetary stations (AISs) started in this country.

V G Kurt, E N Mironova Astro-Space Center, Lebedev Physics Institute, Russian Academy of Sciences, Moscow, Russian Federation
E-mail: vkurt@asc.rssi.ru

Uspekhi Fizicheskikh Nauk **182** (8) 887–894 (2012)
DOI: 10.3367/UFNr.0182.201208j.0887
Translated by K A Postnov; edited by A M Semikhatov